Application of Optical Measurement Technology in Welding Simulation of Box Complex Structure

Application of Optical Measurement Technology in Welding Simulation of Box Complex Structure

Guizhi Zhang [1,2], Yuanbin Fang [1,2,*] and Shuanlao Dong [1,2]

[1] XCMGJiangsu Xuzhou Engineering Machinery Research Institute, Xuzhou,J S 221004, China

[2] XCMG Xuzhou Mining Machinery Co. Ltd, Xuzhou,J S 221004, China

Corresponding author: fybflying@163.com

Abstract. To verify the correctness of the sample quality and the finite element model, optical measurement technology is applied in this study. Unable to consider the quality of tack welding during the established modeling, a three-dimensional scanner is used to detect box complex structures after welding. The finite element model of box structure is established for the study of welding deformation of box structure with short, multi space and multi staggered distributed weld seam. The accuracy of the model is verified by global detection of the structural parts. The results show that the deformation trend warps at the boundary of the left and right plate and concaves in the center of the plate. The maximum deformation of the vertical plate center is 1.714mm. The bottom pad produces the extruding tendency, and the deformation near two sides of the plate is about 0.51mm, which is greater than that of 0.34mm away from the two sides of the plate. The deformation is not consistent in the front and back sides of the Z plate. The maximum error of the sample parts takes place in the front Z shape plate with an error of -0.03mm~0.12mm. There is a certain size difference under the influence of the welding gap, but it still meets the requirements of the engineering application to eliminate the influence of the welding quality on the deformation measurement. By comparing the results of the simulation and the global measurement of the structural parts, the difference between the vibration seat and the front Z plate has a large difference that is 0.12mm~0.24mm, and the deviation satisfies the requirements of the engineering application, and it can effectively guide the production.

1. Introduction

With the light weight design, the traditional welding process accumulation cannot meet the welding deformation control requirements of large and complex structures, and the research of welding simulation prediction has attracted more and more attention. The accuracy and efficiency of computation are the difficulties restricting welding simulation technology. Faced with this common problem, experts at home and abroad have studied the size of finite element models, thermal properties of materials, and thermal loading methods. It can be used to predict the deformation of a large-scale engineering structure to ensure the high precision and efficiency of the model calculation, such as a reasonable grid transition, suitable material high temperature performance parameters and so on.

Non-contact measurement aided with subsequent image processing technology [1] mostly adopts optical measurement, and has been applied more and more in recent years. Based on stereoscopic vision and close range photogrammetry, Liu J. W. et al. [2] used two CCD cameras as image sensors to continuously photograph the continuous deformation image sequence on the surface of the welding parts. The image processing and 3D reconstruction were performed in real time. The target tracking

and the deformation amount were calculated to get any time during the welding process. The deformation field information and the whole deformation dynamic process were carved out. For the optical measurement method, He H. W. et al. [3] used a three-dimensional laser scanner to measure the deformation of butt specimen, drilled and placed precisely the steel ball on the plate. The plate and the steel bead were scanned before and after the welding, and the corresponding point cloud files were output. By using the software of Imageware, the displacement of the measuring point was obtained through coordinate transformation, surface fitting and projection calculation to calculate the angular deformation and bending deformation of the measuring points.

Above all, it is difficult to consider the influence of tack welding quality to the finite element model. Usually, it is assumed that the tack welding quality has no effect on the deformation, and the design of a three-dimensional model is used to establish the model. However, in actual production, the tack welding quality is inconsistent, so it is necessary to detect the quality of the incoming parts. Only the key size is detected, and the accuracy of the overall size cannot be guaranteed.

In this paper, on the basis of the research on the welding deformation of the ironing plate of a paver with 153 welded joints, a total length of 13837mm and the staggered spatial distribution of the staggered paver, a finite element model of the ironing plate is established and welding deformation can be effectively predicted. Three dimensional laser scanning and other measuring techniques are used to analyze the tack welding quality of box structure, and the validity of the finite element model is verified and analyzed from the trend of deformation.

2. Methodology and Methods

The material is Q345 steel. Q345 steel has excellent mechanical properties and good weld ability at room temperature. The box structural ironing plate is made by carbon dioxide gas shielded welding. The welding power is the Fronius 5000. The welding wire is ER50-6 and the diameter of the welding wire is 1.2mm. The form of the ironing plate is shown in Figure 1.

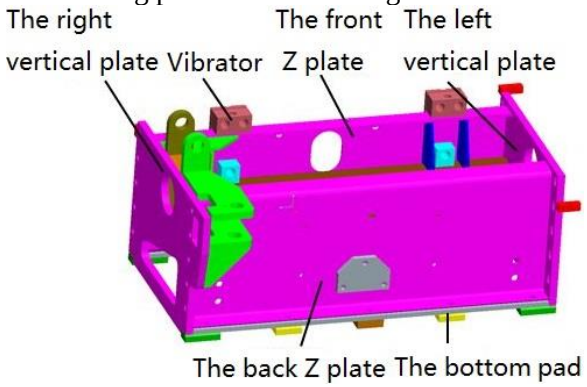

Figure 1. The form of the ironing plate.

A three-dimensional laser scanner is used to measure the outer contour of the ironing plate, and the global deformation is obtained. The relative displacement of the outer contour is used to describe the welding deformation based on the relative shape of the data before and after the welding. The ironing plate is placed on the special welding platform and pasted the reflective spot. It is used the GO Scan 3D scanner to scan. With the aid of LED projector and CCD camera equipment, the specific grating stripe is projected to the outer surface of the ironing plate. The grating interference fringes are photographed. The data information [4] is quickly obtained, and the complete point cloud on the surface of the ironed flat is constructed.

To simulate the welding deformation of the ironing plate, the heat source input is first considered, and the macro metallographic analysis of the weld seam is used to determine the parameters of the heat source. The joint specimen is taken unilateral or bilateral welding into account to measure the weld seam size.

3. Modelling and results

3.1. The establishment of material parameters.

In this research, the grid transition is carried out as 1:2 and 1:3, and the eight node hexahedron element is adopted. The mesh of weld seam is 3mm, and the mesh size far away from the weld seam is about 10mm. The grid model is 389166, and the minimum value of Jacobi is 0.4.

On the view shown in Figure 1, after hiding the ironing component grid, all weld seams are got, as shown in Figure 2. The spatial layout of weld seam is explained according to the coordinate system of XYZ. The weld seams along the Z direction can be divided into three levels: upper, middle and lower. The upper layer is mainly weld seam of vibrator and the front Z plate. The number of weld seams is 12, and the length of weld seam is 1138.95mm. The middle layer is mainly weld seam between the lining plate and the front and back Z plate. The number of weld seam is 31, and the length is 2351.57mm. The lower layer is mainly weld seam of the front and back Z plate, the bottom pad and the long strip. The number of weld seam is 27. The length is 1910.48mm. The weld seam along the Y direction can be divided into three levels: front, middle and back. The front is mainly weld seam of the left and right plate and the back Z plate. The number of weld seam is 14, and the length is 1685.45mm. The middle is mainly the internal partition board and the right vertical plate and so on. The number of weld seam is 7. The length is 593.74mm. The back is mainly the left and right vertical plates and the front Z plate. The total number of weld seam is 16, and the length is 2142.98mm. The weld seam along the X direction can be divided into three levels: left, middle and right. The left is mainly weld seam between the bottom pad and the right vertical plate. The number of weld seam is 16, and the length is 1386.54mm. The middle is the internal partition board and the reinforcing plate, the lining plate and the left and right plate. The number of weld seam is 13, and the length is 1139.90mm. The right is mainly weld seam between the lining plate, the bottom pad and the left vertical plate. The total number of weld seam is 17, and the length is 1487.39mm. It can be seen from the filled grid of all the weld seams that there are many intermittent and complicated spatial orientation.

3.2. The establishment of related parameters.

With reference materials [5], the related parameters of Q345 steel for simulated materials are obtained. Thermal and mechanical properties are varied with temperature. The double ellipsoid heat source model is considered to be the most reasonable heat source model for carbon dioxide gas shielded arc welding.

To avoid rigid body displacement, the rigid position is selected in the constraint condition. At the bottom pad, the surface is set up on the contact plane of the platform. A number of nodes are selected in the middle position of the front and back Z plates to limit the direction of Y and Z. A number of nodes are selected on the bottom of left and right vertical plates to limit the X direction.

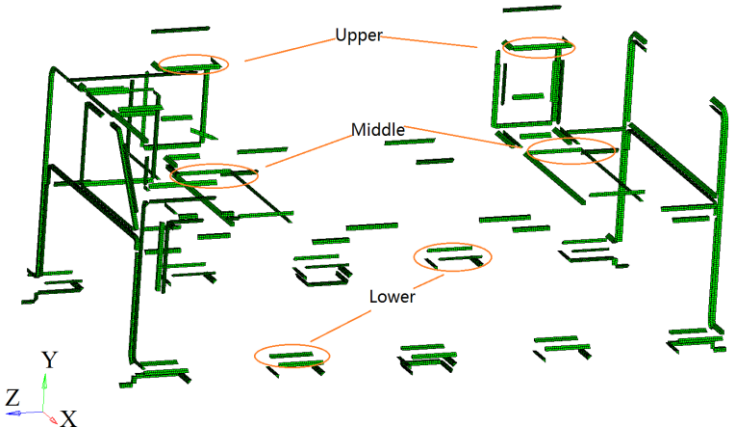

(a) The weld seam along the Z direction

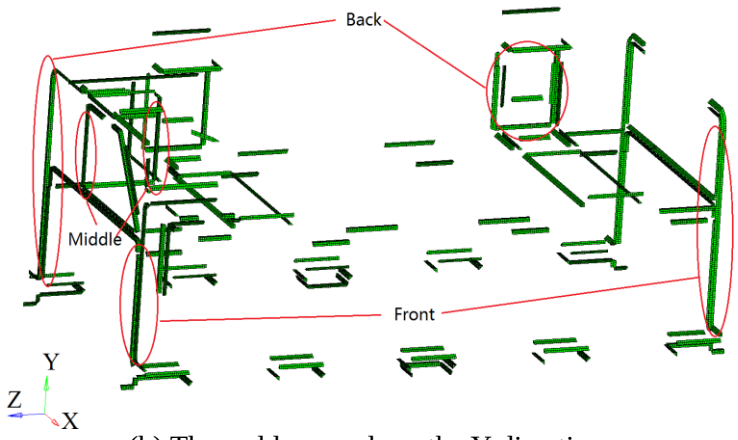

(b) The weld seam along the Y direction

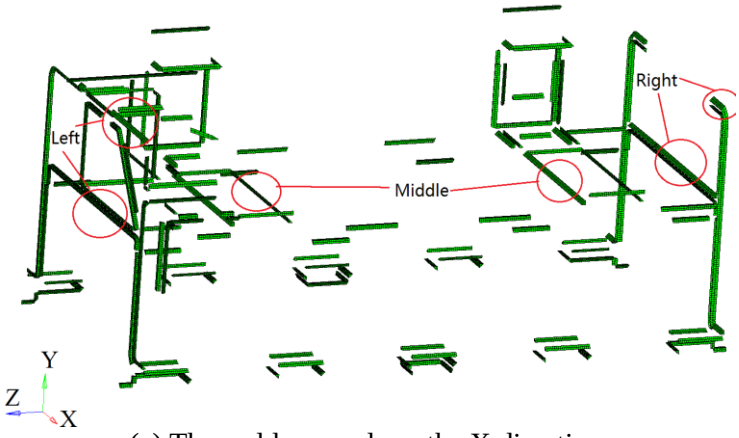

(c) The weld seam along the X direction

Figure 2. The weld seam distribution.

3.3. Simulation results analysis for box structure.

As the finite element model of the ironing plate, the distribution trend of the overall deformation is calculated, as shown in Figure 3.

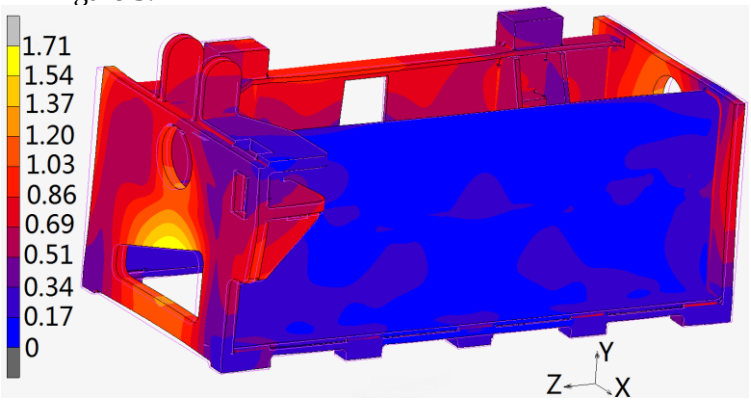

Figure 3.Welding deformation distribution (mm)

From Figure 3, the overall trend is the maximum deformation at the center of the left and right vertical plate with the peak value of 1.71mm. The bottom pad deformation of the left and right vertical plate is about 0.51mm, which is bigger than that of the middle position that is about 0.34mm. At the same time, it can be seen that the maximum deformation value of the front Z plate that is 0.51mm, which is smaller than the maximum deformation value of the back Z shape plate that is 1.2mm. The left and right plates are warped. The deformation of the plate center is concave mainly

due to the contraction of the internal weld seam and the external non welding balance. The bottom deformation is mainly due to the force of the middle lining and the left and right vertical plates, the middle lining and the front and back Z plates, leading to the outer convex trend of the bottom pad. The upper deformation is concave, due to the internal contraction deformation of the articulated free edge position. The deformation of the front and back Z plates is asymmetrical, which is due to the absence of symmetrical welding and the difference of cooling sequence. The deformation trend of the upper and lower vibrator ends is different, due to the different welding directions.

4. Discussion

4.1. Tack welding quality analysis and verification of box structure.

Three-dimensional scanner is used to scan the sample after welding, and then compared with 3D assembly model. Geomagic qualify software is used to analyze and deal with the tack welding precision of the ironing plate. The least squares method is used to fit the two models. The results are compared with the trend of welding deformation, as shown in Figure 4.

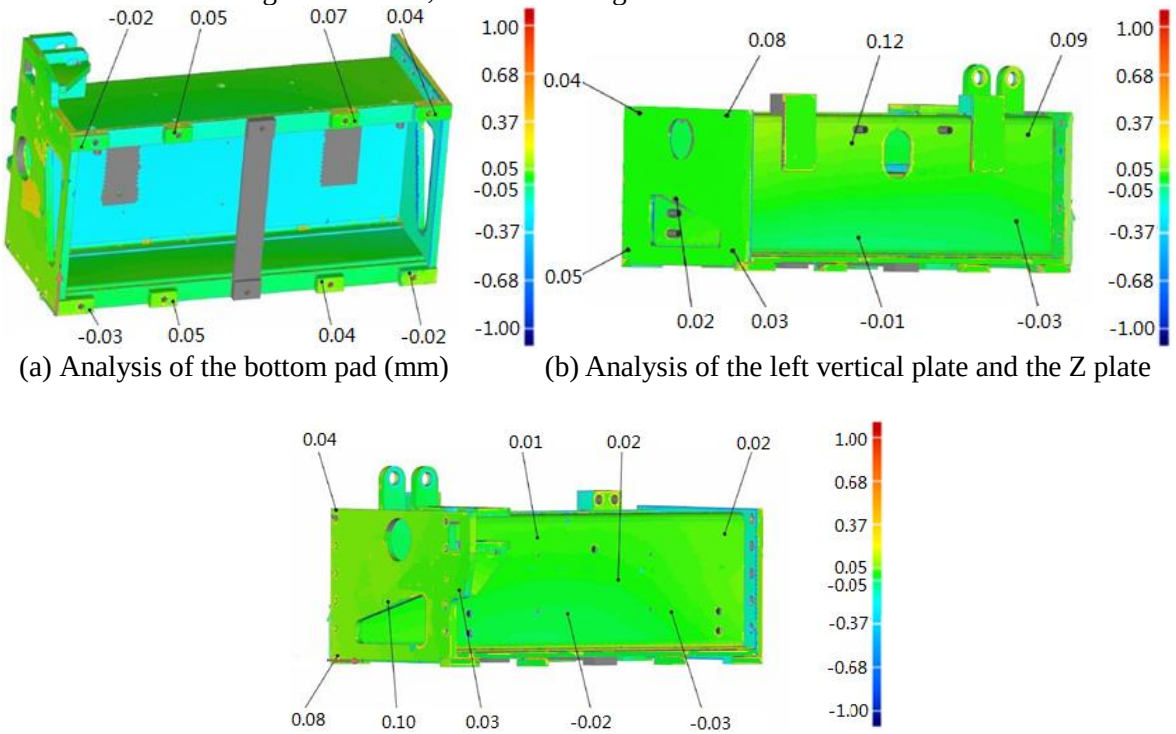

(a) Analysis of the bottom pad (mm) (b) Analysis of the left vertical plate and the Z plate

(c) Analysis of the right vertical plate and the Z plate (mm)

Figure 4. Comparison and analysis results of the tack welding scanning and 3D model.

From Figure 4 (a), the maximum difference deformation of each bottom pad is selected, and the difference between the results of the scanning and the 3D model varies between -0.03mm~0.07mm. From Figure 4 (b), it can be seen that the difference between the left vertical plate and the Z plate has a large difference, and the difference between the results of the scanning and the 3D model varies between -0.03mm~0.12mm. From Figure 4 (c), it can be seen that the difference between the right plate and the Z plate, and the difference between the results of the scanning and the 3D varies between -0.03mm~0.10mm. The large deviation between the left and right vertical plates is due to the unavoidable gap between the tack welding process of the joint between the left and right vertical plates and the Z plates. The straightness of the Z plate and the flatness of the two vertical plates will have a great influence on the precision of the tack welding. However, the tack welding precision of the ironing plate is better. The precision can be satisfied from the overall deformation precision.

4.2. Comparison and analysis of the overall deformation trend.

By the test results, the simulation results of the ironing plate are transferred to the HyperMesh by the method of reconstruction, and the surface elements of all the grids are extracted. The surface mesh is dispersed into the form of triangular facets. In the Geomagic qualify, the least squares method is used to fit the two models, and the results are compared with the trend of the overall welding deformation. The plane with poor agreement is chosen to analyze and explain, as shown in Figure 5.

From Figure 5, the overall deformation trend is the maximum deformation at the center of the left and right vertical plate with the peak value of 1.71mm.

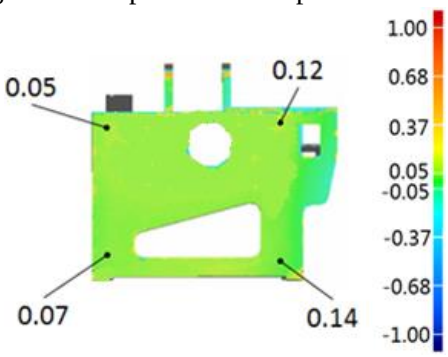

(a) Comparison results of the right vertical plate (mm)

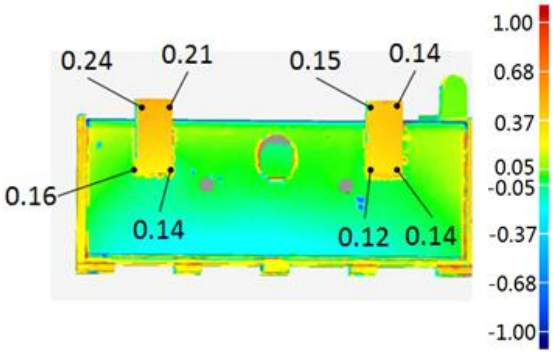

(b) Comparison results of the vibrator (mm)

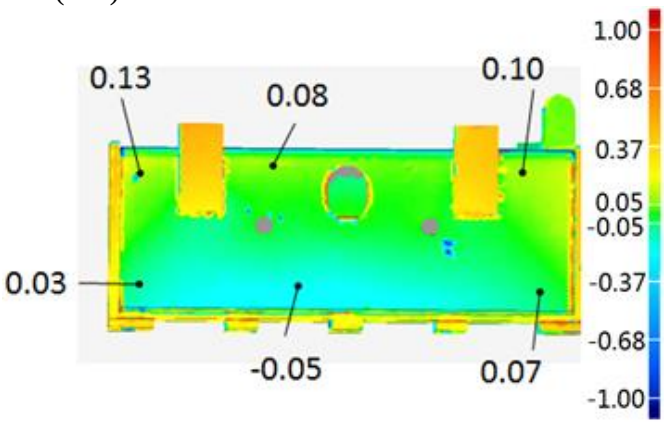

(c) Comparison results of the Z plate (mm)

Figure 5. Contrast between the results of the scan and the simulation results.

From Figure 5 (a), the difference value of the right vertical plate is chosen, and the difference between the results of the scanning and the simulation results is changed between 0.05mm~0.14mm. The results are in good agreement. The difference of the right vertical plate on one side of the front Z plate varies between 0.05mm~0.07mm. The difference of the right vertical plate on one side of the back Z plate is between 0.12mm~0.14mm. The reason that the latter has a larger deviation may be that the partition is the small components before the body welding of the ironing plate, and the components are leveling. The process is shaped and then welded with the ironing plate.

From Figure 5 (b), it can be seen that the difference value between the vibrator and the front Z plate is larger, and the difference of the vibrator varies between the 0.12mm~0.24mm. The deviation of the vibrator is large because the vibrator is welded after the main body of the ironing plate. The difference of the right and left vibrators varies between 0.14mm~0.24mm and 0.12mm~0.15mm. The difference is mainly related to no symmetrical welding and the tack welding accuracy between the vibrator and the front Z plate.

From Figure 5 (c), the difference value of the vibrator and the front Z plate is chosen, and the difference of the front Z plate varies between the -0.05mm~0.13mm. The negative deviation is mainly related to the datum defined by the model fitting algorithm, and the trend of deformation is still the

same. The difference of the front Z plate is changed between 0.08mm~0.13mm. The deviation is mainly related to the bending spring-back of the front Z plate, and the simulation results cannot consider the bending spring-back factor. The difference of the front Z plate varies between -0.05mm~0.07mm. The deviation is related to the bending spring-back of the front Z plate, but also the welding precision of the bending plate, the long strip, the bottom pad and the left and right vertical plate.

By comparison, the plane with good agreement between the scanning result and the simulation result can effectively prove the correctness of the prediction results.

5. Conclusions

In this paper, the finite element model of box structure with complex space weld seams is established, and the welding deformation distribution is predicted. Three-dimensional scanner is used to detect the welding quality of box structure. On the basis of the welding quality to meet the production requirements, the welding deformation of box structure is measured. The simulation results are compared and analyzed to verify the correctness of the finite element model.

Through the study, the following conclusions are drawn: the edge position of the left and right plate is warped, and the center position is concave. The maximum deformation occurs in the center of the vertical plate. The bottom pad is "drum" deformation. The deformation of the front and back Z plate is not consistent. The size difference of box structure is affected by the tack welding gap of the steel plate, but it need to examine and meet the requirements of engineering application. By comparing the simulation results and measurement results, the deviation error meets the requirements of engineering application. And it can effectively guide production. From the view of engineering application, the further optimization research needs to be further verified by the optical measurement technology.

Acknowledgments

This work was financially supported by Jiangsu Natural Science Foundation (BK20180175) and Jiangsu Natural Science Foundation (BK20180176).

References

[1] Cai Z P, Lu A L, Shi G K, Zhao H Y and Shi Q Y 2001 *J. Mech. Eng.* **37**(2): 62-65.
[2] Koke I, Müller W H, Ferber F, Mahnken R and Funke H 2008 *Compos. Sci. Technol.* **68**(5): 1156-1164.
[3] Xu D, Zhang Y B, Liu C G, Xie Z M and Li X. 2014 *Mar. Tech.* (3): 42-46.
[4] Fang Y B, Zong X M, Xiao Y, Zhou P X, Liang J and Yin X Q 2016 S *Elec. Weld. Mach.* **46**(8): 17-21.
[5] Fang Y B, Zong X M, Zhang H Q, Yin X Q and Zhang L J 2017 *T. Chin. Weld. I.* **38**(8): 45-49.